Computers and Chemical Engineering 96 (2017) 87–102

Contents lists available at ScienceDirect

Computers and Chemical Engineering

journal homepage: www.elsevier.com/locate/compchemeng

Bi-level optimizing operation of natural gas liquefaction process

Wangyun Won [a,1], Jiyong Kim [b,*]

[a] Plant Research Team, GS Engineering & Construction, 33, Jong-ro, Jongno-gu, Seoul 110-121, Republic of Korea
[b] Department of Energy & Chemical Engineering, Incheon National University, 119, Academy-ro, Yeonsu-gu, Incheon 406-772, Republic of Korea

ARTICLE INFO

Article history:
Received 2 February 2016
Received in revised form 15 October 2016
Accepted 19 October 2016
Available online 20 October 2016

Keywords:
Natural gas
Liquefaction
Refrigeration
LNG
Optimizing control

ABSTRACT

The production of liquefied natural gas (LNG) is a highly energy intensive process, as required liquefaction temperature is approximately −160 °C at atmospheric pressure. In this study, we propose a novel bi-level optimizing operation system for an LNG process, which consists of a real-time steady-state optimizer (RTSSO) and a decentralized control system. The RTSSO computes the optimal operating conditions such that the compressor power is minimized, while the decentralized control system performs real-time feedback actions to attain the target operating points against various disturbances. Special attention was given to the decentralized control system so that i) the process operation can be rapidly stabilized, and ii) the developed system can be seamlessly applied to an actual process. The performance of the proposed operation system was validated in a numerical LNG plant that precisely replicates an actual plant that produces 100 t of LNG per day.

1. Introduction

Natural gas (NG) is the fastest growing fossil fuel. Worldwide, the total consumption of NG is anticipated to increase by nearly 70% between 2002 and 2025 (EIA, 2005). There are several stimulators for this growth that mainly originate from its clean properties, *i.e.* approximately half of the CO_2 emissions of conventional coal power generation, minimal SO_x and NO_x emissions, and the introduction of carbon price policies (Gómez et al., 2014; Kumar et al., 2011; Taylor et al., 2012). Large amounts of NG are found in remote locations where pipeline transportation in gaseous phase is infeasible or uneconomical (Lee et al., 2012; Moein et al., 2015). Thus, in many cases, transporting liquefied NG (LNG) by ships is preferred (Park et al., 2016; Won et al., 2014). The liquefaction of NG facilitates the shipment as the volume is reduced by a factor of 600 (Kumar et al., 2011).

The LNG production process (hereafter, referred as LNG process for simplicity) consists of expensive and delicate pieces of equipment, such as compressor and cold box, and so stabilizing process operation is an important issue in real industrial plants (Jensen and Skogestad, 2009). In addition, because the required liquefaction temperature is approximately −160 °C at atmospheric pressure (Mortazavi et al., 2012), utility management such as heat and electricity is also a crucial issue for LNG producers to secure competitiveness (EIA, 2003).

Similarly to other chemical processes such as distillation (Lei et al., 2013; Mizoguchi et al., 1995; Rewagad and Kiss, 2012), crystallization (Aamir et al., 2010; Ma et al., 2002; Nagy and Braatz, 2012), simulated moving bed (Abel et al., 2005; Natarajan and Lee, 2000; Klatt et al., 2002), and batch-wise reactors (Kiparissides et al., 2002; Lee et al., 1999; Seo et al., 2007; Won et al., 2009, 2010), the stability and economics of the LNG process can be greatly improved by introducing an optimal operation system. However, published works on this subject appear to be limited. The majority of studies reported to-date has focused on the design issues, including energy analysis (Kanoğlu, 2002; Li and Ju, 2010; Morosuk et al., 2015; Remeljej and Hoadley, 2006; Vatani et al., 2014), alternative process configuration (Chang et al., 2011; Kikkawa et al., 1997; Lee et al., 2012; Wang et al., 2012), heat exchanger design including refrigerant type optimization (Aspelund et al., 2010; He and Ju, 2014; Khan et al., 2013; Khan and Lee, 2013; Lee et al., 2002; Nogal et al., 2008; Xu et al., 2013), and dynamic modeling of cryogenic systems (He and Ju, 2016; Rodríguez and Diaz, 2007; Singh and Hovd, 2007). Only few groups have aimed at developing energy-thrifty operation system for a simple refrigeration cycle (Jensen and Skogestad, 2007a,b) and simplified commercial LNG processes (Husnil et al., 2014; Michelsen et al., 2010) focusing on the decentralized control technique. No published literatures have demonstrated efforts towards optimizing control of a realistic industrial LNG plant.

* Corresponding author.
E-mail address: jykim77@incheon.ac.kr (J. Kim).
[1] Current address: Department of Chemical and Biological Engineering, University of Wisconsin-Madison, Madison, WI 53706, USA.

http://dx.doi.org/10.1016/j.compchemeng.2016.10.009
0098-1354/

Nomenclature

d	Disturbance
E	Compressor power consumption
g	Constraint

Abbreviation

CV	Controlled variable
DOF	Degree of freedom
HMR	Heavy-key mixed refrigerant
IMC	Internal model controller
JT	Joule-Thomson
LMR	Light-key mixed refrigerant
LNG	Liquefied natural gas
MCHE	Main cryogenic heat exchanger
MR	Mixed refrigerant
MV	Manipulated variable
NG	Natural gas
PID	Proportional-integral-derivative
RNGA	Relative normalized gas array
RTSSO	Real-time steady-state optimization
WEDT	Warm end delta temperature

Symbols in control structure

FC	Flow controller
FFC	Flow fraction controller
HC	Hand controller
LC	Level controller
LS	Low selector
PC	Pressure controller
PPC	Compression ratio controller
SC	Speed controller
TC	Temperature controller
TDC	Temperature difference controller

Accordingly, the objective of this study is to propose a novel bi-level optimizing operation system for the LNG process. The operation system consists of two major parts: the real-time steady-state optimizer (RTSSO) and the decentralized control system composed of multiple PID controllers. The RTSSO, whenever invoked, determines new optimum operating points. Special attention is paid to develop the sophisticated decentralized control system that runs continuously and conducts the regulation of process. We develop two separate control systems, where each is dedicated to liquefaction and refrigeration units, in addition to the integrated control system that can solve the energy imbalance issues that arise when controlling the liquefaction and refrigeration units independently.

The performance of the proposed operation system is validated in a numerical 100 ton-per-day LNG plant, which is delicately developed to replicate an actual plant in Incheon, Korea. It serves as not only an operating training system but also as the testing site for the new operation system so that it can be seamlessly implemented to the actual plant. Therefore, all detailed features of the actual plant, such as safety interlock logics and operational constraints of equipment and instrument, are precisely reflected in the numerical plant.

2. Process description

Fig. 1 shows the process flow diagram of the 100 ton-per-day LNG plant being constructed in Incheon, Korea. In this plant, the Korea Single Mixed Refrigerant (KSMR) cycle which was developed and patented by Korea Gas Corporation (KOGAS) was adopted as a liquefaction process (Lee et al., 2013). Among the process sections, the liquefaction and refrigeration units to cool and liquefy NG require the largest amount of energy.

Table 1
Design conditions for the LNG process.

Condition		Value
LNG temperature at the exit of MCHE (°C)		−150.7
Feed gas temperature (°C)		12.1
Feed gas pressure (bar)		63.4
Feed gas composition	Nitrogen	0.0496
	Methane	0.8690
	Ethane	0.0510
	Propane	0.0213
	i-Butane	0.0044
	n-Butane	0.0045
	i-Pentane	0.0001
	n-Pentane	0.0001

As illustrated in Fig. 1, there are two major process circuits in liquefaction and refrigeration units: NG circuit and mixed refrigerant (MR) circuit. Each is described separately.

The pre-treated NG from feed gas intake facility is a mixture of nitrogen, methane, ethane, propane, butane, and pentane at approximately 63.4 bar and 12.1 °C as given in Table 1. It is cooled to −16.3 °C as it passes through the top bundles of main cryogenic heat exchanger (MCHE). The scrub distillation (SD) column performs two main functions: (i) the removal of heavy hydrocarbons to avoid freezing at the cold end of the MCHE and (ii) the recovery of ethane and propane for refrigerant make-up. The bottom product of SD is routed to the fractionation section for further separation into ethane, propane, butane, and heavier hydrocarbons. The vapor overhead from SD is partially condensed at the middle bundle of MCHE before being fed to scrub distillation reflux drum (SDRD), where vapor and liquid are separated. The vapor is then sent to the bottom section of MCHE and is reduced at a temperature below −150 °C, which causes the NG to be liquefied. The LNG is then sent to separator SR3 through the control valve V3. The bottom liquid of the separator SR3 is pumped to LNG storage tank, while the boil-off gas from the top is used as a fuel or otherwise routed to flare header.

The MR circuit is a closed refrigeration loop that supplies the cooling demands to MCHE. The MR is composed of nitrogen, methane, ethane, and propane. It is pressurized by a series of compressors that are driven by independent motors and operate at different speed. The pressure of MR reaches approximately 52.5 bar inside separator SR2. The liquid and vapor from SR2 consist mainly of heavy and light components, respectively. The heavy-key MR (HMR) is sub-cooled through the top bundle of MCHE and then is let down in pressure through Joule-Thomson (JT) valve V1. This low pressure stream reenters MCHE as a cooling medium and provides the cooling demand to pre-cool feed gas and light-key MR (LMR) from SR2. In addition, this stream sub-cools the HMR from SR2 and is finally superheated at the end of the MCHE. The fully vaporized MR is then recycled to the compressor CP5. The LMR from SR2 is condensed and sub-cooled in MCHE. It exits at the cold end of MCHE and is reduced in pressure across the JT valve V2. This low pressure stream is then completely vaporized and superheated by exchanging heat with the NG streams and with LMR and HMR from SR2. Finally, it is returned to the compressor CP1.

Two independent temperature controllers that manipulate the bypass valves V4 and V5 are installed to adjust the degrees of feed gas pre-cooling and SD condenser cooling. All the compressors are centrifugal types and are equipped with the anti-surge recycle line (dashed lines in Fig. 1), suction drum, and fan-type discharge cooler. The anti-surge valves are manipulated by independent safety control logic. A distributed control system from Yokogawa Co. is used

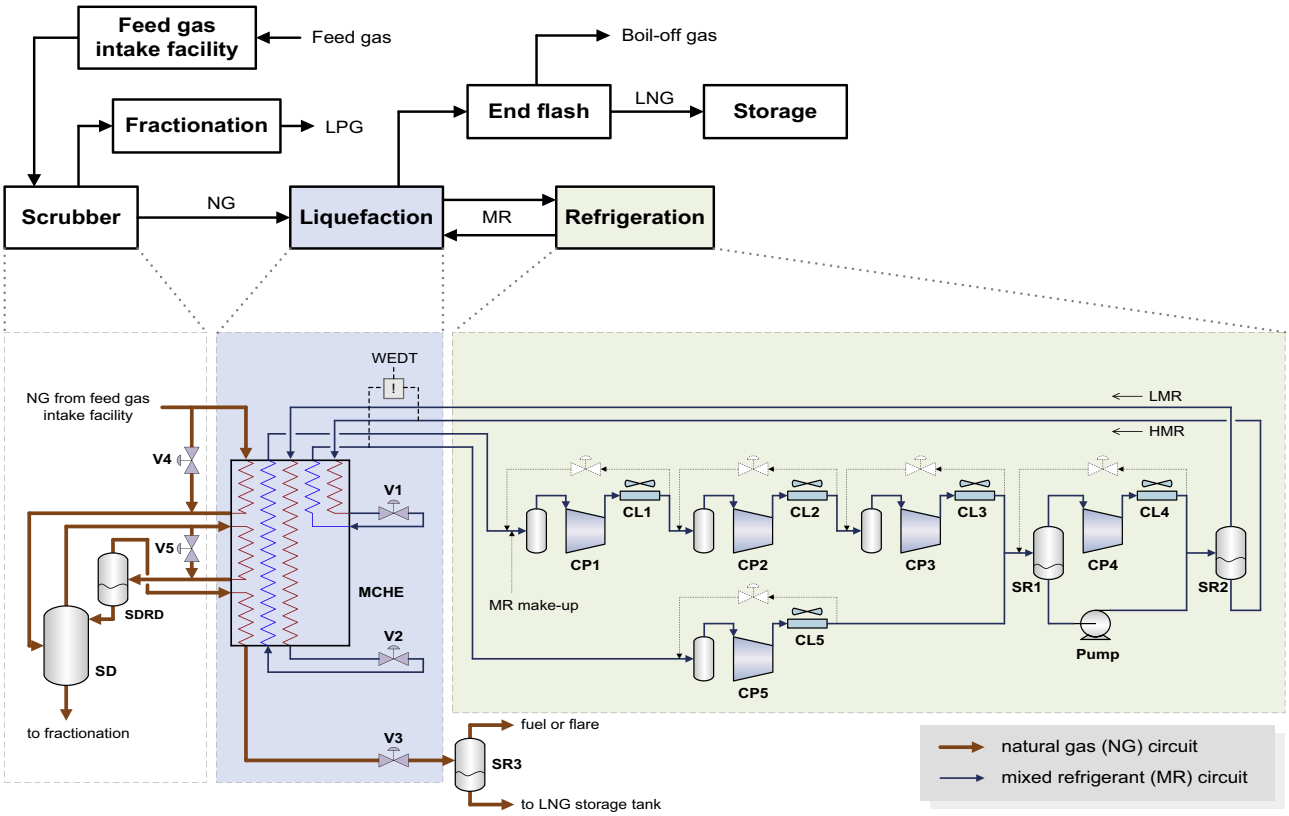

Fig. 1. A process flow diagram of the key process units in the LNG plant. CP: compressor, CL: cooler, MCHE: main cryogenic heat exchanger, SD: scrub distillation, SDRD: scrub distillation reflux drum, and SR: separator.

for receiving and transmitting field signals, safety interlock logics, and local controllers.

The operation system should be developed in a feasible form under the environment described above. The key design conditions are summarized in Table 1.

3. Process model development

Rigorous steady-state and dynamic models are developed using Aspen HYSYS. The entire design data of actual plant, such as piping and instrument diagram, cause and effect diagram, plot plan, datasheet for equipment and instruments, and various vendor prints, are all reflected in these models. The key parameters including compressor performance curves are corrected using shop test data supplied by manufacturers.

4. Optimizing operation system

4.1. Overall structure

Fig. 2 shows the overall structure of the proposed bi-level optimizing operation system. The operation system consists of two major parts: the real-time steady-state optimization system and the decentralized control system. The optimization system computes the optimum compression ratio for compressors CP2, CP3, and CP4 and the optimum warm end delta temperature (WEDT) using process measurements and process model such that the cost function is minimized. The optimum values are provided to the decentralized control system as target values and are pursued by local controllers. Each part of the optimizing control system will be described in more detail.

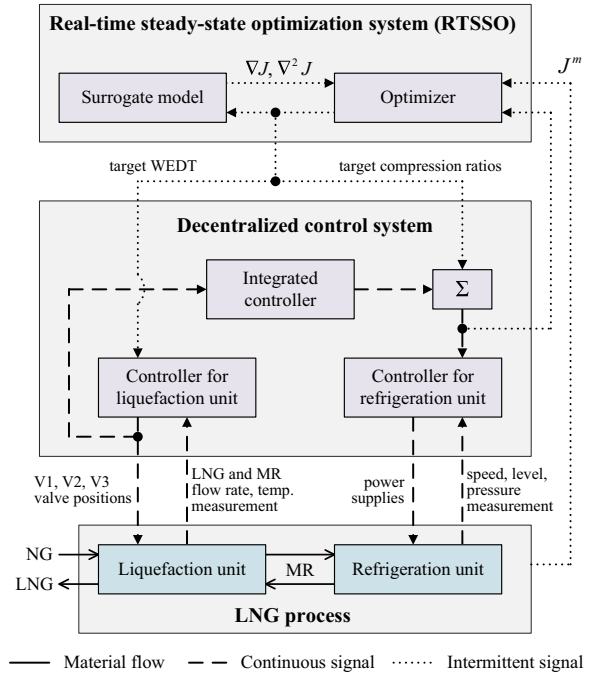

Fig. 2. Overall structure of the bi-level optimizing control system.

4.2. Decentralized control

4.2.1. Design philosophy and degrees of freedom analysis

The primary purpose of refrigeration unit is to provide constant compression energy to MR, while the primary goal of liquefaction unit is to produce LNG at desired flow rate and temperature by using

the energy supplied from refrigeration unit. To achieve these aims while stabilizing the process against various disturbances, we first developed two independent control systems that are dedicated to the liquefaction and refrigeration units, respectively, using multiple PID controllers. Then, we developed the integrated control system that balances energy supply and demand of the above two units, so that the energy loss can be minimized and uncontrollable status can be avoided.

Following the rules suggested by Jensen and Skogestad (2009), the degree of freedom (DOF) for liquefaction and refrigeration units is analyzed. The results are summarized in Table 2. The anti-surge valves and the suction drums for compressors CP1, CP2, CP3, and CP5 are not considered in this analysis because they are introduced for abnormal conditions. In contrast, the level of two flash drums SR1 and SR2 have steady-state effects. In other words, we can utilize the MR composition and active charge as DOF by controlling the levels, and hence we count them in actual steady-state DOF. Here, the active charge is defined as the total mass of refrigerant accumulated in the MR circuit, *i.e.* mainly in the heat exchangers. In the considered units, the number of DOF with no steady-state effect is zero, as marked by asterisk in Table 2.

The liquefaction and refrigeration units have three and eleven actual steady-state DOFs, respectively. These DOFs can be exploited to obtain better process performance or to stabilize the operation against disturbances and set point changes.

4.2.2. Control of liquefaction unit

Three DOFs listed in Table 2 for liquefaction unit can be used to control three controlled variables (CVs). The LNG flow rate and temperature should be selected as CV by pairing with V1, V2, or V3 because they are directly related to the specification of LNG product (LNG production rate and heating values). The remaining one DOF may be directly used for operation optimization. However, better strategy is to form a control loop with WEDT, which is defined as temperature difference between HMR from SR2 and HMR to CP5, in order to improve the process responses.

Fig. 3 illustrates the proposed control system for liquefaction unit. Particularly, flow fraction control (FFC) is adopted to enhance the dynamic characteristics of closed loop, and in addition, override control is employed to produce LNG that meets product spec for the insufficient cooling duty. The details are described below in a step-by-step manner.

4.2.2.1. Input-output pairing. The control system for liquefaction unit consists of three parallel PID controllers working together. Each controller can manipulate one of the manipulated variables (MVs) to control one of the CVs. However, since multiple streams exchange heat simultaneously in a cold box, the interaction among MVs and CVs is very complicated, and the pertinent relationships between variables are unclear.

In order to determine the most appropriate input-output pairs, we employed relative normalized gain array (RNGA) method that considers not only the process steady-state information but also the transient information (Hu et al., 2010). For this, we first conducted step response experiments in the dynamic model described in Section 3 and then approximated each input-output pairs with a first-order plus dead time (FOPDT) model by using area-based method (Åström and Hägglund, 1995; Bi et al., 1999) such that

$$G(s) = \begin{bmatrix} \frac{0.074}{151.5s+1} & \frac{0.040}{262.7s+1} & \frac{-0.022e^{-9.2s}}{414.6s+1} \\ \frac{-5.88\cdot 10^{-5}\cdot e^{-76.9s}}{28.7s+1} & \frac{-4.84\cdot 10^{-5}e^{-83.3s}}{35.8s+1} & \frac{0.350}{10.5s+1} \\ \frac{-0.012e^{-119.5s}}{4918.4s+1} & \frac{-0.029e^{-90.3s}}{4607.7s+1} & \frac{0.109e^{-33.6s}}{388.7s+1} \end{bmatrix} \quad (1)$$

In Eq. (1), the columns of the matrix represent the outputs: WEDT, LNG flow, and LNG temperature, sequentially; the rows indicate the inputs: valve positions of V1, V2, and V3, in order. Based on this model, the RNGA, Λ_N, is computed as

$$\Lambda_N = K_N \otimes K_N^{-T} = \begin{bmatrix} 1.137 & -0.137 & -\varepsilon \\ \varepsilon & -\varepsilon & 1.000 \\ -0.137 & 1.137 & -\varepsilon \end{bmatrix} \quad (2)$$

where $\otimes$ denotes the element-by-element multiplication, and ε represents a very small number. K_N indicates a normalized gain array, which elements are calculated by dividing steady-state gain by average residual time. The steady-state gain and average residual time are obtained from the transfer function matrix in Eq. (1). Here, the average residual time is defined as the sum of time constant and dead time of the FOPDT model.

Seborg et al. (2010) recommends that the CVs and MVs be paired, so that all paired RNGA elements are positive and are closest to one. Therefore, we select V1 to control the WEDT, V2 to control the LNG temperature, and V3 to control LNG flow. The performance of controllers designed based on the FOPDT model in Eq. (1) is demonstrated in the result section in detail.

4.2.2.2. Flow fraction control. One of the features of the proposed control system is the replacement of an ordinary flow controller (FC) by a flow fraction controller (FFC) in a cascade control loop.

Fig. 4 compares the information flow of the two control systems, where the one adopts an FC and the other one employs an FFC. It is expected that any changes in LNG flow will ultimately cause changes in the refrigerant flow as long as LNG temperature is maintained constant. In the control system presented in Fig. 4(a), this manipulation of refrigerant flow rate is accomplished by a feedback controller TC that manipulates the set points of the inner-loop FC. Under this control system, relatively long transient response of LNG temperature before stabilized is not unavoidable due to slow dynamics of heat exchanging process between MR and LNG. On the other hand, the control system in Fig. 4(b) is capable of immediately adjusting the refrigerant flow rate against the variation of LNG flow rate; FFC increase or decrease the refrigerant flow rate proportionally to the LNG flow rate. This instantaneous feedforward-like action reduces the effect of changes in LNG flow rate on the LNG temperature. As a result, the LNG temperature can be stabilized more quickly than the case with FC.

In practical implementation, the denominator of the flow ratio is amended as max (LNG flow, δ) for small number δ, as shown in Fig. 3, in order to avoid numerical errors.

The FFC for the HMR flow was designed in a similar manner.

4.2.2.3. Override control. Sudden increase in LNG flow may cause the severe increase in LNG temperature, which may result in the failure to meet the product spec and excessive generation of boil-off gas from SR3. To avoid such issues, we introduced a low selector LS01 and a temperature controller TC01 that overrides the output of hand controller HC01 when the LNG temperature approaches its upper bound. The maximum allowable temperature of LNG is given to TC01 as set point.

It should be noted that the primary purpose of override control is to produce on-spec LNG in any cases, particularly when the MR cold duty is insufficient to cool and liquefy the entire NG. In normal operation, *i.e.* the case that sufficient cold duty is supplied and LNG temperature is kept closely to the desired target value, HC01 overrides the output of TC01 through LS01 and dominates the flow control loop of FC01 such that the LNG is produced at a target flow rate.

4.2.3. Control of refrigeration unit

A compressor is an expensive and delicate piece of equipment, so the stability of the process operation should be the highest pri-

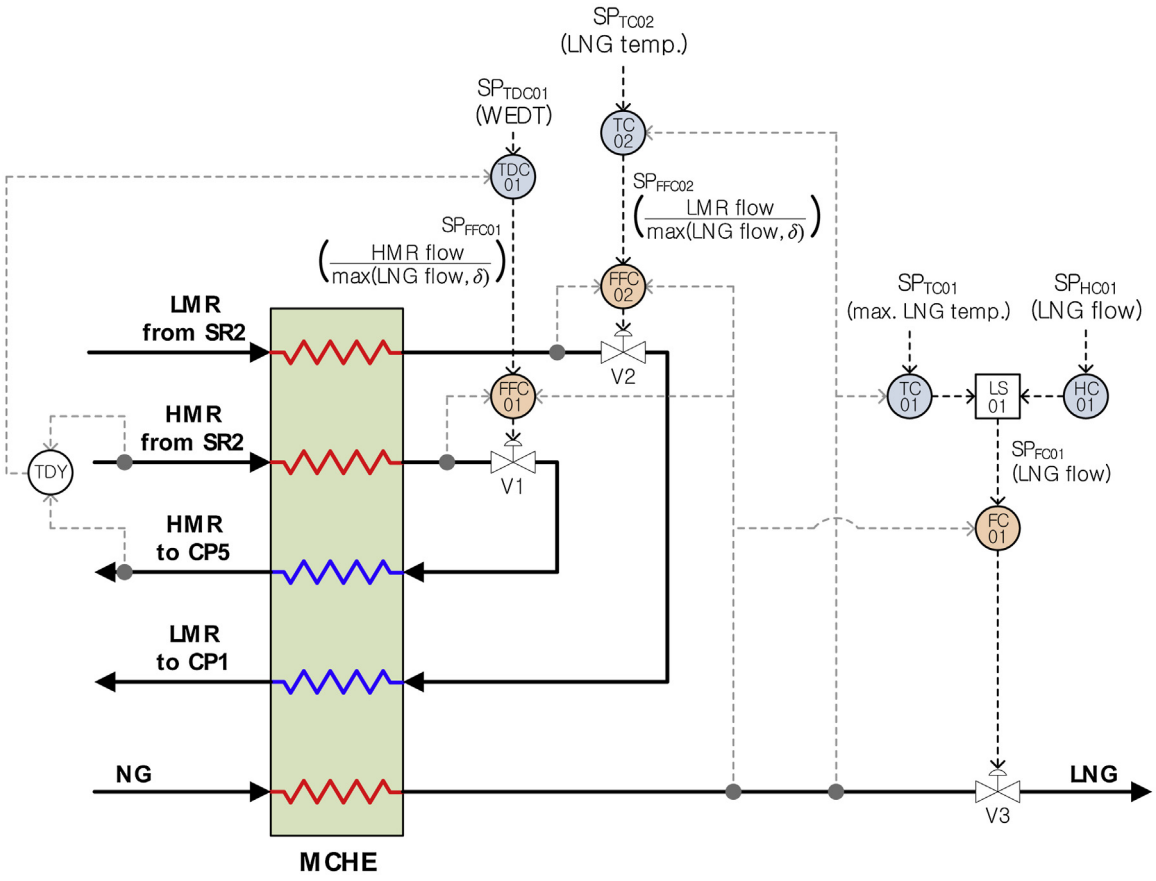

Fig. 3. Control system for liquefaction unit. The filled circles indicate relevant measurement.

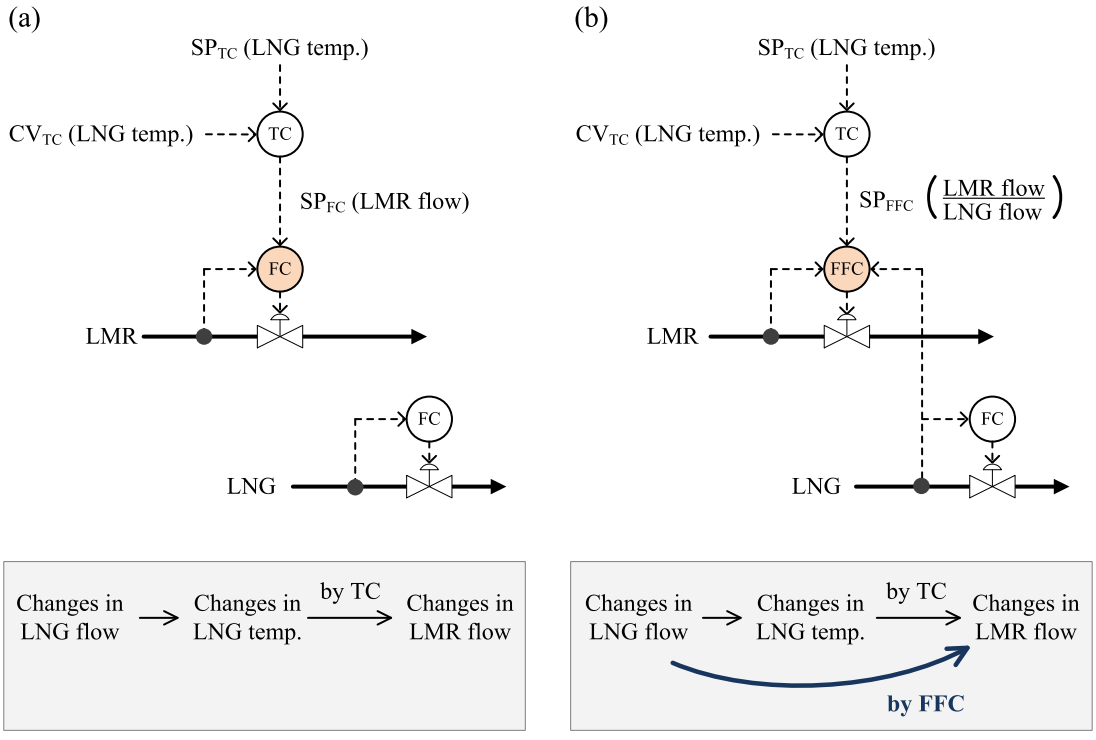

Fig. 4. Comparison between (a) flow control and (b) flow fraction control.

Table 2
Degrees of freedom analysis.

Liquefaction unit			Refrigeration unit		
				Compressor power (CP1-CP5)	5
	LNG valve position (V3)	1		Pump power (Pump)	1
+	Choke valve position (V1, V2)	2	+	Discharge-cooler power (CL1-CL5)	5
	MVs	3		MVs	11
–	MVs with no steady-state effect	0[a]	–	MVs with no steady-state effect	0[a]
=	Actual steady-state degrees of freedom	3	=	Actual steady-state degrees of freedom	11

[a] The number of degrees of freedom (level tanks) with no steady-state effect is zero.

ority in controller design. This is in accordance with the industrial practice. The control loop using eleven DOFs in Table 2 is determined in this manner. The control system for refrigeration unit will be described in more detail according to the types of DOF.

4.2.3.1. Five compressor powers. Each of the five compressor powers can be paired with three alternative CVs: suction pressure, discharge pressure, and compression ratio between inlet and outlet streams. Because all the compressors are interconnected in a closed circuit, their operation affects one another. In this circumstance, controllers may be in conflict with each other, depending on the selection of CVs and their set values. For instance, one controller that controls the discharge pressure of a compressor may be failed to achieve its set point if the preceding compressor is operated at very low speed (by other controller) and so the inlet pressure is not maintained high enough. To avoid these problems, we decided to use CP1 and CP5 powers to control CP1 and CP5 suction pressures, respectively, and to use CP2, CP3, and CP4 powers to control the compression ratio of corresponding compressors, respectively. The detailed control scheme is illustrated in Fig. 5. In this figure, anti-surge recycle lines, compressor suction drums, and fan-type discharge coolers that were introduced in Fig. 1 are omitted for simplicity.

Another alternative is to use CP4 power to control CP4 discharge pressure and to use remaining compressor powers to control their respective compression ratios. In this design, the pressure at the inlet of choke valves are maintained constant while the pressure downstream of the choke valves may vary depending on the control actions of TDC01 and TC02. However, we could find that pressure at the outlet of the choke valves has more significant effect on the JT effect than the inlet pressure, for the given MR composition and the pressure drop across the valves; in order to obtain sufficient cooling of MR *via* JT expansion, the outlet pressure of choke valves should be kept at a low level. Therefore, we selected to control the suction pressure of CP1 and CP5, which are closely related to the outlet pressure of choke valves V1 and V2.

Pressure controller, PC02, and two low selectors, LS02 and LS03, are introduced to protect the downstream vessel and pipe lines from being subjected to pressures that exceed their design limits. PC02 overrides the output of PPC01 and PPC02 when the outlet pressure of CP3 approaches its design limit. The control output of PC02 is multiplied by α, which is defined as the speed ratio of CP2 to CP3, before transferred to LS02 so that the compressor loads are distributed evenly between CP2 and CP3. Similarly, the override control loop for CP4 is provided with PC03 and LS04.

In order to enhance the process response, the speed controllers, SC01 to SC05, that are cascaded from each pressure controllers are employed.

4.2.3.2. Five discharge-cooler powers. The remaining five fan-type heat exchangers in Table 2 are used to regulate the outlet temperature of each compressor. This is to reduce drift caused by temperature changes and let subsequent equipment operate in a benign environment. The suggested design of these controllers is provided in Appendix A.

4.2.3.3. One pump. There are two adjustable holdups, *i.e.* SR1 and SR2, in closed MR cycle. Thus, one of them must be controlled to avoid overfilling or emptying of tanks. We decided to use the pump downstream of SR1 to control the liquid level of SR1. In addition, flow controller is introduced as an inner loop control to prevent the process from drifting away from its desired operating point on the short time scale. The detailed design of these control loops is presented in Appendix A.

4.2.4. Integrated control of liquefaction and refrigeration units

In this section, we first describe the motivation for developing integrated controller and then present the specific strategy and algorithms.

4.2.4.1. Necessity of integrated control. The position of choke valves V1 and V2 are determined by the feedback controllers in Fig. 3, on the way to trace the target values of WEDT and LNG temperature, respectively. However, more radically, the valve positions are determined by the energy balance between refrigeration and liquefaction units. This is because the energy supplied to refrigeration unit is used to liquefy NG in liquefaction unit. For example, if small compression energy is supplied to the refrigeration unit, TDC01 and TC02 would increase the MR flow rate by more opening JT valves, so that sufficient cooling duty can be provided to MCHE and LNG can be produced at correct quality and conditions. On the other hand, if large amount of energy is supplied to refrigeration unit and therefore MR is highly compressed, the controllers would open less the choke valves since a small amount of MR is enough to cool and liquefy NG.

If energy supply and demand are severely imbalanced between these two units, JT valves become almost fully open or close. This may cause the instability of process operation as follows:

- Case 1: less energy is provided to compressors than required in MCHE. In this case, choke valves become fully open. However, as shown in Fig. 6, the MR cold duty rather decreases with increased valve opening beyond a certain point. This is because the absolute changes in flow rate and the MR temperature *via* JT expansion decrease as the choke valve position increases. The controller will fail if the sign of process gain changes with operating condition, as observed in this case.

Here, the cold duty is a cooling demand that can potentially be used for NG cooling *via* heat exchange in MCHE. The cold duty is proportional to MR flow rate and temperature difference across JT valves.

- Case 2: more energy is provided to compressors than consumed in MCHE. In this case, choke valve positions approach zero. This causes the reduction of MR flow that returns to CP1 and CP5, and as a result, the compressors fall into unstable surge condition, which may cause mechanical damage (#1 in Fig. 7).

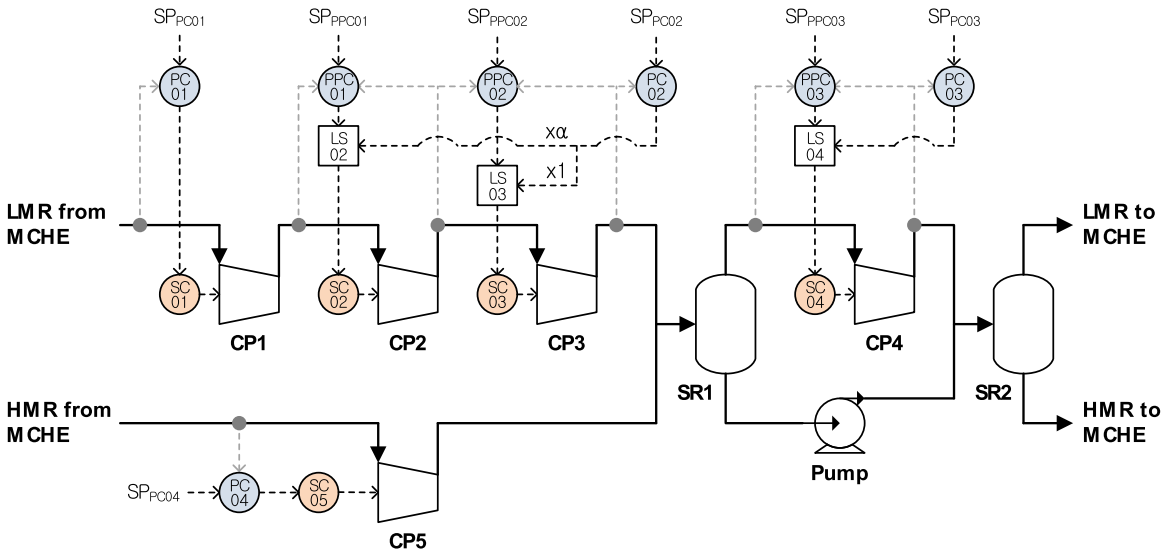

Fig. 5. Control system for refrigeration unit. The filled circles indicate relevant measurement.

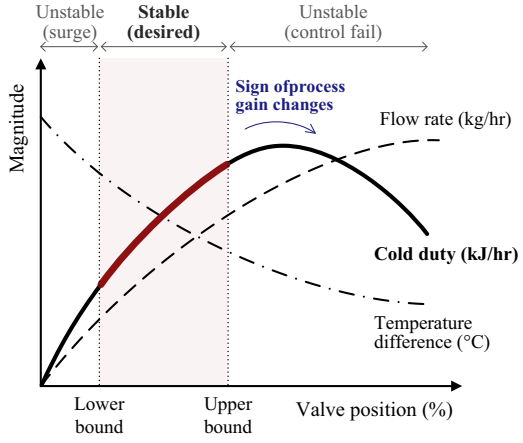

Fig. 6. MR cold duty, flow rate, and temperature difference across the choke valve according to the valve position for the fixed compressor power.

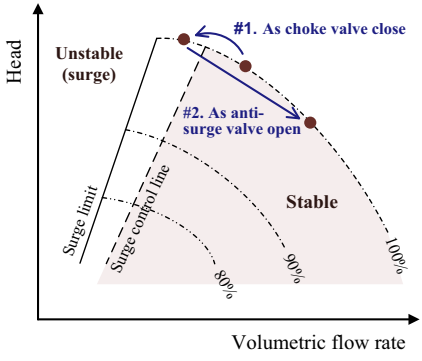

Fig. 7. Movement of operating point on a compressor performance map when more energy is supplied to the system than required. Filled circles indicate operating points.

Anti-surge valves may open to protect the compressors (#2 in Fig. 7). However, the opening of anti-surge valves is the process to dissipate the surplus energy through throttling loss, which apparently means energy-waste.

In short, there exists a stable operation range of JT valve that is desired to be kept in during operation.

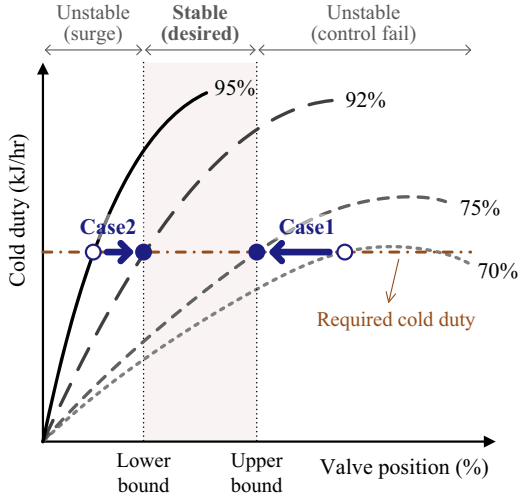

Fig. 8. Refrigerant cold duties according to the compressor powers and choke valve position. Hollow and filled circles indicate present and target operating points, respectively, and percentages represent compressor powers.

The stable range of JT valve can be considered as constraints during steady-state optimization. However, in actual plant, this may be easily violated due to disturbances. Therefore, it is needed to devise a control system that can continuously draw JT valves into stable range *via* coupled operation of two systems, *i.e.* liquefaction and refrigeration units.

4.2.4.2. Operational strategy and principle. Fig. 8 shows the MR cold duties according to the compressor powers and choke valve position. The required cold duty is determined by feed gas conditions, such as flow rate, pressure, and temperature. As illustrated in this figure, choke valve position can be indirectly adjusted by manipulating compressor power. This is because the feedback controllers, TDC01 and TC02, modify the choke valve positions such that equal amount of cold duties can be provided to MCHE against changes in compression energy.

Based on this principle, we developed the integrated control system. This system balances the energy between refrigeration and liquefaction units. If the choke valve position is in the prescribed stable range, the integrated controller does not take any actions. However, if the choke valve position drifts away from the stable

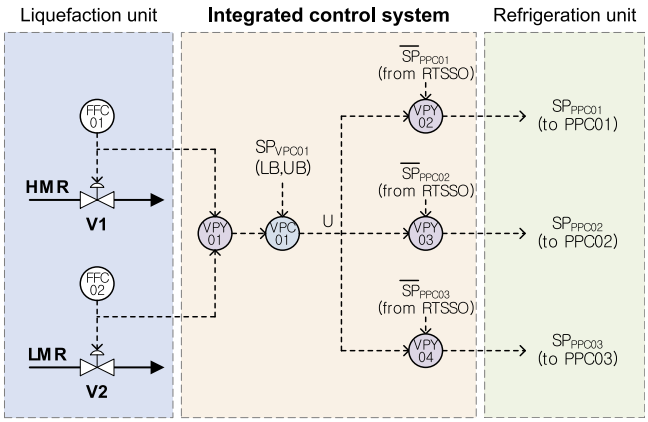

Fig. 9. Integrated control system for liquefaction and refrigeration units.

region, it starts to manipulate the compressors. During the control, the upper bound (Case 1) or lower bound (Case 2) of the stable range is used as a target value, so that the operating point is not too much drifted apart from the conditions computed by optimizer by the action of integrated controller.

4.2.4.3. Control structure and implementation procedure. Fig. 9 shows the detailed structure of the integrated control system. Based on the choke valve positions computed by FFC01 and FFC02, the control system corrects the set points of PPC01, PPC02, and PPC03, which were calculated by RTSSO. Because it is important to maintain the pressure downstream of choke valves below an adequately low level to secure sufficient JT cooling of MR, the set points of PC01 and PC04 are not utilized as MVs for this control system.

Fig. 10 explains the implementation procedure of integrated control system. Steps 1 to 3 are conducted by VPY01, and step 4 is carried out by VPC01 in Fig. 9. The last step 5 is taken by three calculation blocks, VPY02 to VPY04 in Fig. 9.

First, the positions of two choke valves, V1 and V2, are obtained. Second, control errors are calculated by using the lower or upper bound of the stable region as set point. In this step, control errors are set to zero if the choke valve is in the predefined stable range. Third, based on the absolute control errors, one of two choke valves is selected to be controlled. In the fourth step, control output of integrated controller is computed. Since excessive movement of compressor set points will likely upset the process too much, only the I-controller, *i.e.* integral action of PID controller, is used for this calculation. Based on the control output, the compression ratio set points provided by RTSSO are updated in the final step. In this step, the current operating speed of compressors is multiplied to the control output, so that the compressor load can be distributed evenly among compressors during manipulation.

It is noteworthy that we revised the set points offered by RTSSO by adding appropriate correction factors, as shown in step 5 in Fig. 10, rather than replacing them with completely new values. By doing this, we can move the compressor operations, which are driven by independent motors and run at different speed, all in a uniform direction when adjusting them by integrated controller, so that the control effects do not cancel each other out.

It is also noteworthy that the integrated controller does not consume any DOFs since it uses the identical DOFs to the pressure ratio controllers PPC01, PPC02, and PPC03.

4.3. Real-time steady-state optimization

In the previous section, we proposed a decentralized control system that regulates the process using the DOFs listed in Table 2. It should be noted that no DOFs are lost by the decentralized con-

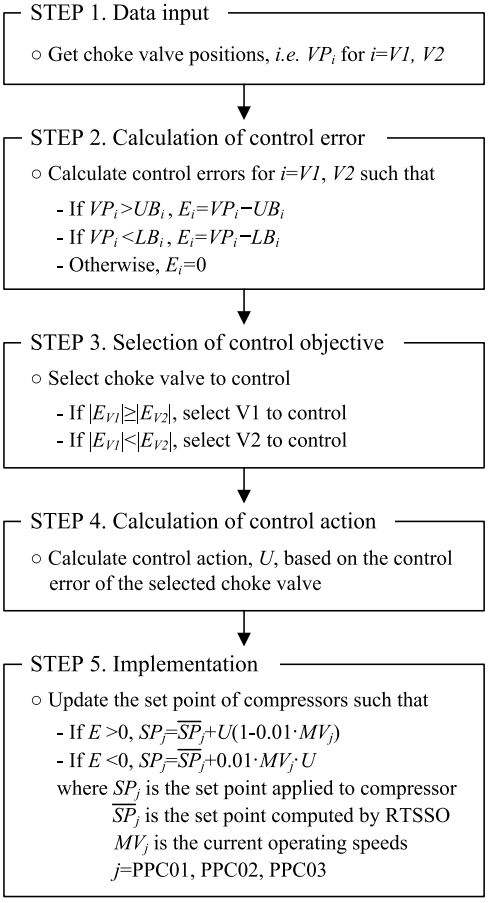

Fig. 10. Implementation procedure of integrated control system.

trollers since their set points replace the manipulated inputs as DOF; the set points of stabilizing level loops remain DOF for the upper layer. In this paper, we utilized these set points for the operation optimization to improve the process performance.

Table 3 summarizes the primitive DOFs and their substitutes under proposed decentralized control system. The set points of PC01 and PC04 are fixed at a predefined value rather than being re-optimized, in order to secure sufficient cooling of refrigerant through JT expansion. The set points of TC03 to TC07 and LC01 are also fixed during operation so that subsequent rotating equipment can operate in a constant condition. Because the LNG flow rate and temperature are generally determined by market condition and price, *e.g.* changes in the required LNG heating value, the set points of HC01 and TC02 are not used for operation optimization as decision variables. The remaining set points of PPC01, PPC02, PPC03, and TDC01 are optimized by RTSSO in Fig. 2.

The optimizer, whenever invoked, computes the optimum operating condition for a given disturbance d such that

$$\min_{\varphi} J = \sum_{j=\text{CP1-CP5}} E_j(\varphi, d) \text{ subject to } g(\varphi, d) \le 0 \quad (3)$$

where E denotes the operational energy consumed by the compressors CP1 to CP5, and φ indicates the decision variables that consist of set points of PPC01, PPC02, PPC03, and TDC01. The constraints function g defines the safety and operational limits of equipment/instruments as well as the interlock logics, such as emergency shutdown, process shutdown, and compressor vendor shutdown, considered in the actual plant. Particularly, the stable operational range of choke valves, discussed in Section 4.2.4, is also reflected as constraints during optimization.

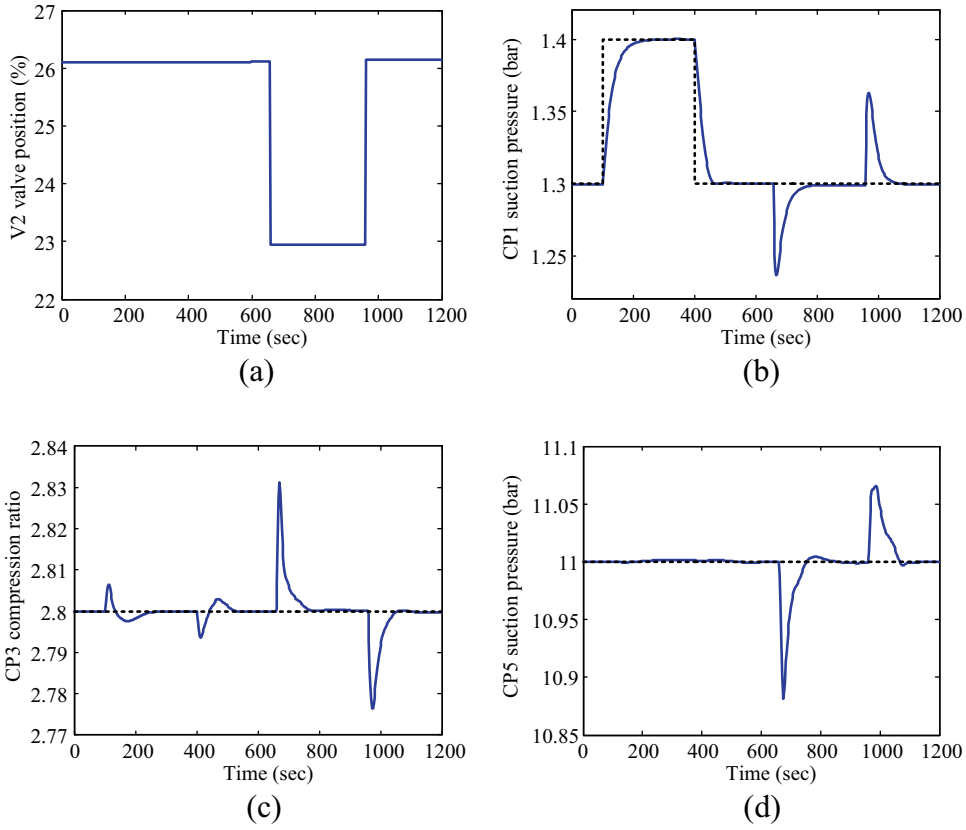

Fig. 11. Results of control against set point change in CP1 suction pressure and temporary change in V2 valve position; (a) V2 valve position, (b) CP1 suction pressure (PC01), (c) CP3 compression ratio (PPC02), and (d) CP5 suction pressure (PC04). The dotted lines indicate set points.

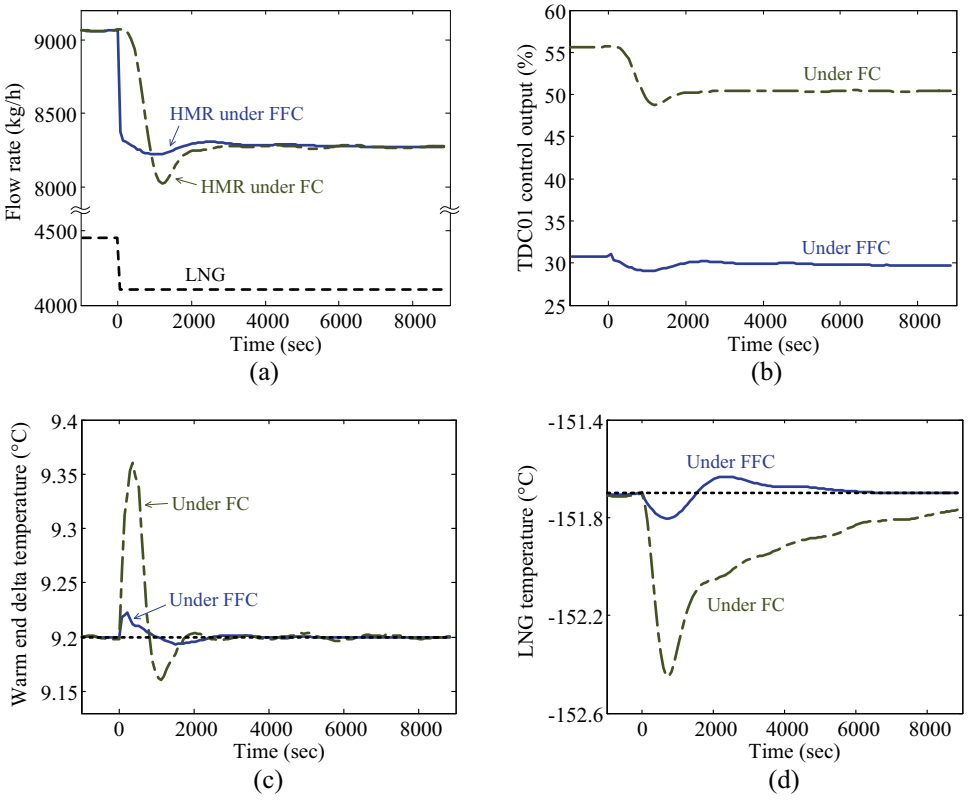

Fig. 12. Performance comparison of two control systems for liquefaction unit, where each employs flow control and flow fraction control, respectively, as a lower-layer controller in a stabilizing cascade loop; (a) LNG and HMR flow rates, (b) control output of TDC01, (c) response of warm end delta temperature (TDC01), and (d) response of LNG temperature (TC02). The dotted lines indicate set points.

Table 3
Degrees of freedom under proposed control system.

Section	Primitive manipulated inputs	Substitute	Status
Refrigeration	CP1 power	Set point of PC01	Fixed
	CP2 power	Set point of PPC01	Need to be optimized[a]
	CP3 power	Set point of PPC02	Need to be optimized[a]
	CP4 power	Set point of PPC03	Need to be optimized[a]
	CP5 power	Set point of PC04	Fixed
	CL1 fan power	Set point of TC03	Fixed
	CL2 fan power	Set point of TC04	Fixed
	CL3 fan power	Set point of TC05	Fixed
	CL4 fan power	Set point of TC06	Fixed
	CL5 fan power	Set point of TC07	Fixed
	Pump power	Set point of LC01	Fixed
Liquefaction	V1 valve position	Set point of TDC01	Need to be optimized[a]
	V2 valve position	Set point of TC02	User-defined[b]
	V3 valve position	Set point of HC01	User-defined[b]

[a] It will be determined through real-time steady-state optimization.
[b] It will be provided by operator.

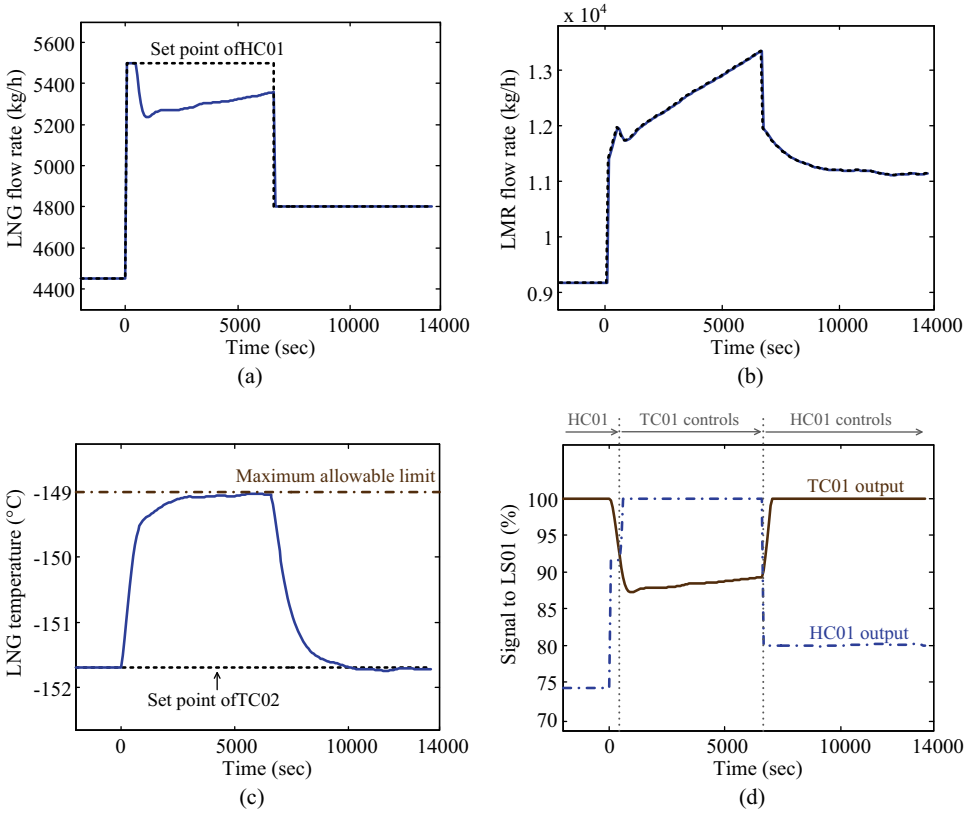

Fig. 13. Results of control against set point change in LNG flow rate; (a) controlled response of LNG flow rate (FC01), (b) controlled response of LMR flow rate (FFC02), (c) controlled response of LNG temperature (TC02), and (d) control signal to low selector LS01.

In the implementation, a sequential quadratic programming method was used to solve the above constrained optimization in Eq. (3). The gradient (∇J) and hessian ($\nabla^2 J$) are evaluated using the surrogate model, while the objective function is measured from the LNG process as shown in Fig. 2. The surrogate model is derived from a rigorous steady-state process model as a nonlinear regression model using the principal component analysis and neural network (Lang et al., 2009). MATLAB with ActiveX objects is used to build up this model. This implementation using surrogate model allows us to curtail the computational burden by preventing frequent recourse to original complex model and also enables us to find correct descent direction by avoiding numerical errors incurred by inconsistent convergence of iterative modules in process simulator.

5. Results and discussion

In this section, we first investigate the performance of the proposed operation system in a numerical LNG plant, which precisely replicates an actual plant that produces 100 t of LNG per day, focusing on the effectiveness of featured techniques against various disturbance and set point change scenarios. Then, we compared the performance of the suggested operation system with that of an alternative scheme, which is a slight modification of control scheme suggested by Mandler (2000).

In all simulations, standard PID algorithm, apart from the derivative kick, with IMC tuning is used for decentralized controllers (Skogestad, 2003).

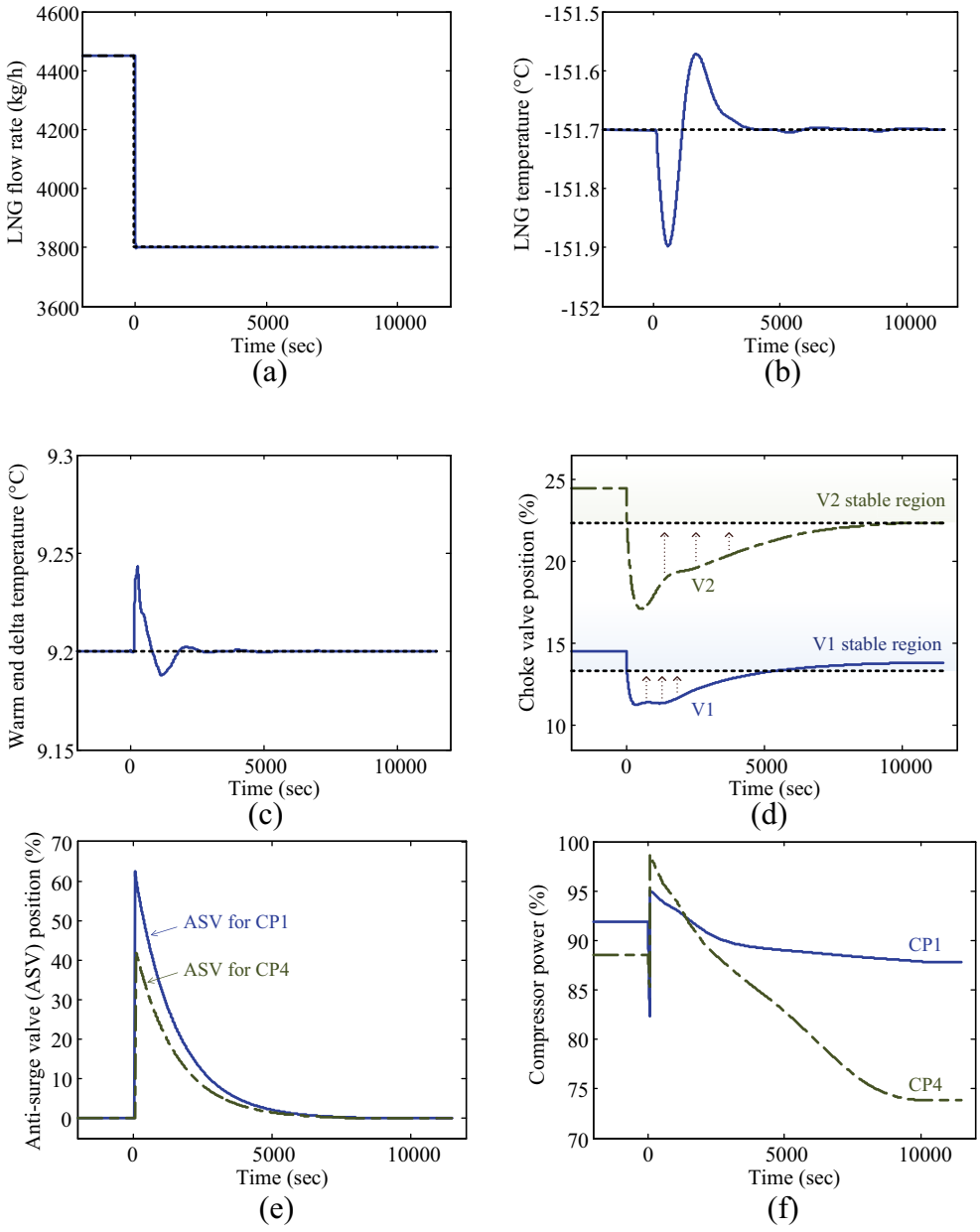

Fig. 14. Performance of integrated control of liquefaction and refrigeration units; (a) LNG flow rate, (b) response of LNG temperature (TC02), (c) response of warm end delta temperature (TDC01), (d) choke valve positions (FFC01 and FFC02), (e) anti-surge valve position (anti-surge controller), and (f) compressor power (integrated controller).

5.1. *Performance of decentralized control system*

5.1.1. *Control of refrigeration unit*

Fig. 11 illustrates the performance of the proposed control system for refrigeration unit. The set points of PC01 (CP1 suction pressure) is changed from 1.3 bar to 1.4 bar at 100 s and then is turned to 1.3 bar after 300 s. The valve position of choke valve V2 is changed from 26.1% to 22.9% at 660 s and is then changed back to 26.1% at 960 s, as a disturbance.

In Fig. 11(b), it is shown that CP1 suction pressure deviates from its set points for a while when the set point change starts, but the controller recovers the suction pressure rapidly after a short transient. In the meantime, the CP3 compression ratio undergoes some deviation from its set points due to the PC01 control action but completely returns to the set point in approximately 100 s of transient, as shown in Fig. 11(c).

It is also observed that CP1 suction pressure, CP3 compression ratio, and CP5 suction pressure show deviations from their set points around 660 s and 960 s due to the changes in V2 valve position but satisfactorily well-settled on the respective set points in a short transient.

It should be noted that the proposed control system stabilized the refrigeration process rapidly without any conflictions between controller constituents.

5.1.2. *Control of liquefaction unit: flow fraction control* versus *flow control*

Fig. 12 shows the results of the two different control systems, where each adopts FC and FFC as a lower-layer controller, respectively, for both TDC01 and TC02 cascade control loop. In order to investigate the superiority of FFC over FC, the LNG flow that has significant effect on the WEDT and LNG temperature, which are the CVs of the master control loops (TDC01 and TC02 in Fig. 3), was changed from 4450 kg/h to 4100 kg/h as disturbance. The step change in the LNG flow is determined such that the control performance of FC and FFC is distinct and in addition the interlock logics

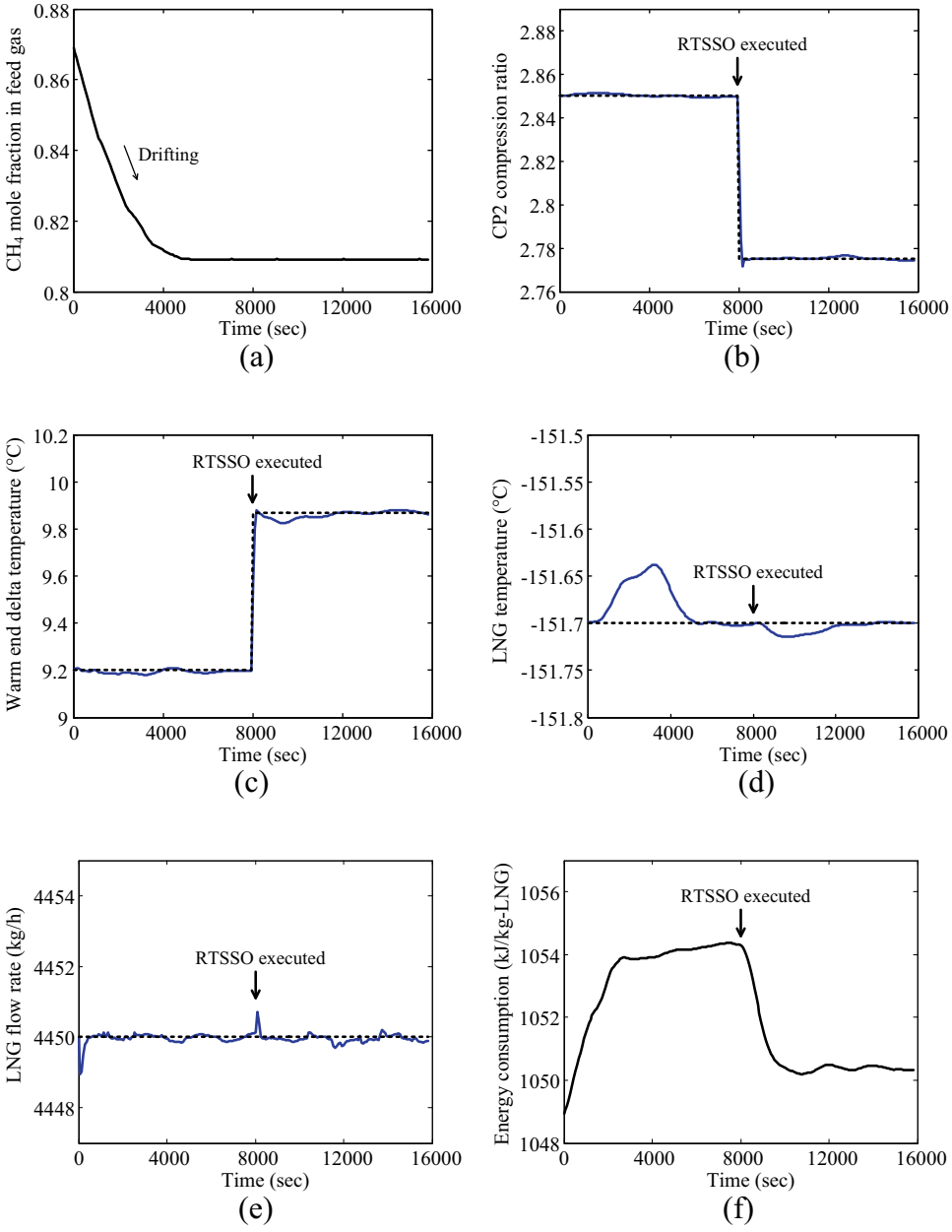

Fig. 15. Results of real-time steady-state optimization; (a) mole fraction of methane in feed natural gas, (b) CP2 compression ratio (PPC01), (c) warm end delta temperature (TDC01), (d) LNG temperature (TC02), (e) LNG flow rate (FC01), and (f) energy consumption. The dotted lines indicate set points.

considered in the numerical plant are not activated during the performance test. In this simulation, the integrated controller was set to manual mode (no control).

In Fig. 12(a), it is shown that HMR flow under FFC is immediately reduced as LNG flow rate decreases. This is because the set point of the FFC is given as a ratio of HMR flow to LNG flow, as described in Section 4.2.2. Since the refrigerant flow rate is instantaneously manipulated in proportion to the LNG flow rate, the deviation of LNG temperature and WEDT from their set points is alleviated, and only minor feedback correction is considered as observed in Fig. 12(b).

In contrast, however, the HMR flow decreases with relatively long dynamics when FC is employed. This is because the refrigerant flow rates in this case are ultimately adjusted by the FC's upper layer feedback controllers, *i.e.* TDC01 and TC02. As a result, WEDT and LNG temperature exhibit considerably long transient response before stabilized, as depicted in Fig. 12(c) and (d), respectively. In addition, in this case, the upper layer controllers are required to take larger feedback control action than the case with FFC, as shown in Fig. 12(b).

5.1.3. *Control of liquefaction unit: override control*

Fig. 13 shows the performance of the proposed control system for liquefaction unit against the sudden increase in LNG flow rate. As the LNG flow rate increases from 4450 kg/h to 5500 kg/h, the LMR flow is also sharply increased by the flow rate controller FFC02, as shown in Fig. 13(b). However, due to the lack of refrigerant cold duty, LNG temperature continuously increases. As the LNG temperature approaches its prescribed upper bound, −149 °C, the control output of TC01 is decreased and eventually become smaller that of the HC01 around 500 s, as observed in Fig. 13(d). As a result, the TC01 overrides the HC01 *via* low selector LS01, and the lower-layer flow control loop FC01 is utilized as a mean to control LNG temperature rather than tracing the target LNG production rate. In Fig. 13(a)

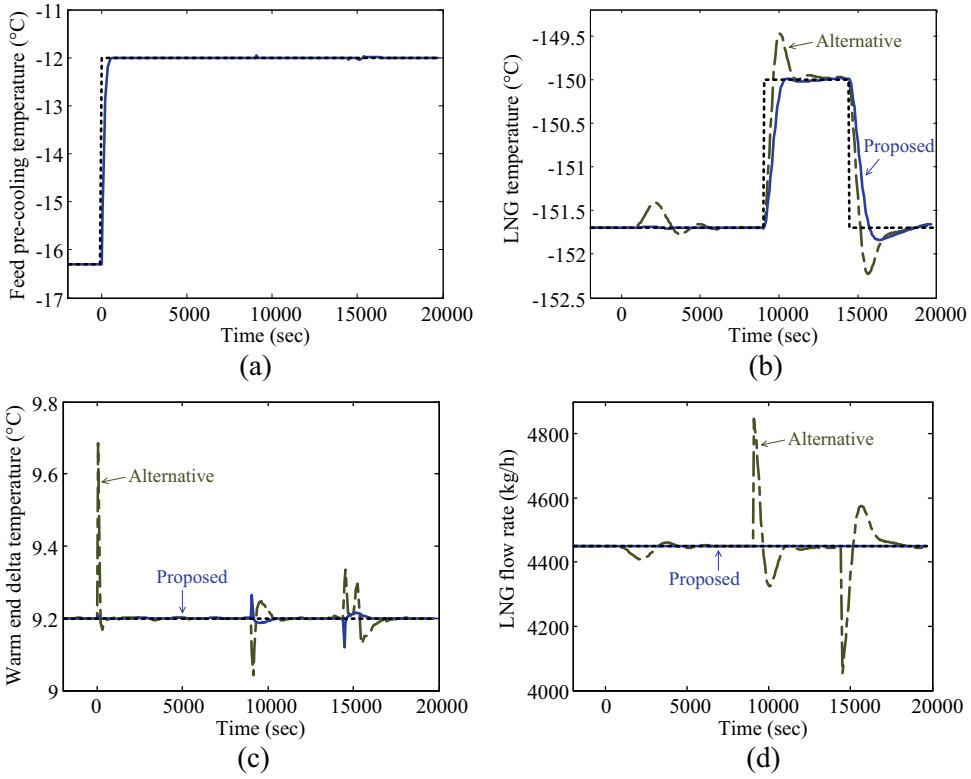

Fig. 16. Performance comparison between the proposed and alternative control schemes; (a) feed pre-cooling temperature, (b) LNG temperature, (c) warm end delta temperature, and (d) LNG flow rate. The dotted lines indicate set points.

and (c), it can be seen that LNG flow rate is reduced so that the LNG temperature does not violate its maximum allowable limit. In the meanwhile, the LMR flow rate is steadily increased by a feedback controller TC01.

At 6600 s, the set point of LNG flow rate is changed once more to 4800 kg/h. Because the refrigerant cold duty is sufficient to cool and liquefy the NG in this case, the LNG temperature is recovered to its target value provided to TC02, and LNG flow rate returns to target production rate given to HC01.

5.1.4. Integrated control of liquefaction and refrigeration units

Fig. 14 displays the performance of the integrated control system for liquefaction and refrigeration units. In order to test the performance of designed controller, we changed the set point of LNG flow rate from 4450 kg/h to 3800 kg/h.

In Fig. 14(a)–(c), it is shown that LNG temperature and WEDT deviate from their respective set points when LNG flow rate starts to decrease. The temperature controllers, TDC01 and TC02, and their lower-layer controllers, FFC01 and FFC02, take an action to stabilize the process, and this leads to a decrease in refrigerant flow rate with decreasing choke valve positions, as observed in Fig. 14(d). The reduction of MR flow rate moves the compressor operations into an unstable surge region, and as a result, anti-surge valves become open, as depicted in Fig. 14(e). In this situation, the integrated controller reduces the set points of pressure ratio controllers to steer the choke valve positions above the predefined lower bounds. This results in a decrease in compressor powers, as shown in Fig. 14(f). As the compressor power decreases, the TDC01 and TC02 gradually increase the refrigerant flow rate to obtain sufficient cold duty with decreasing MR pressure, and this leads to increases in choke valve positions and decreases in anti-surge valves, as observed in Fig. 14(d) and (e), respectively. The decrease in compressor powers continues until all choke valve positions are placed above their lower bounds. Here, the lower bounds of the choke valve positions are determined such that anti-surge valves are completely closed.

It should be noted that the control action of integrated controller consequently restricts the compressor duty to match the reduced inflow of NG.

5.2. Performance of real-time steady-state optimization

Fig. 15 demonstrates the performance of the bi-level optimizing operation system, shown in Fig. 2.

As the CH_4 mole fraction in feed gas drifts apart from its initial value for the first 4500 s, the energy consumption in compressors gradually increases. This is shown in Fig. 15(f). After 8000 s is elapsed, the RTSSO is executed, and the set points for PPC01, PPC02, PPC03, and TDC01 are updated to the optimized values based on the new feed gas composition values. Fig. 15(b) and (c) shows exemplary cases on how CP2 compression ratio and WEDT respond to the new set points, respectively. The developed operation system stabilizes the process quickly against the initial changes in feed gas composition and also against the set points changes by RTSSO execution. As the process operating conditions move to the optimized points, the energy consumption decreases.

5.3. Performance comparison with alternative control system

Fig. 16 compares the performance between proposed and alternative control systems. In order to investigate the disturbance rejection and set point tracking performance, the set point of feed pre-cooling temperature is changed from −16.7 °C to −12 °C at 0 s, and the set point of LNG temperature is changed from −151.7 °C to −150 °C at 9000 s and is then changed back to −151.7 °C at 14,400 s. For the operation of refrigeration unit, the control system presented in Fig. 5 is used for both cases.

Detailed structure of the alternative control system is presented in Appendix B. The main idea for the design of alternative control system is borrowed from Mandler (2000). One feature of this control system is the use of LMR flow rate to control LNG production rate. The change in LMR flow rate causes the change in LNG temperature, which in turn causes the change in LNG flow rate *via* feedback control loop for LNG temperature. The advantage of this mechanism is that refrigerant flow rate is always adjusted in advance before LNG flow rate is manipulated. This enables us to naturally restrict the LNG production rate to meet the target LNG temperature as the first priority.

However, despite the structural advantage described above, the alternative control system exhibits slower responses to disturbance and set point changes than the proposed control system in Fig. 3, which is delicately designed based on the process steady-state and dynamic characteristics, as shown in Fig. 16.

6. Conclusions

In this study, we proposed a novel bi-level optimizing operation system for an LNG process. The proposed structure is composed of an RTSSO that determines the optimal compression ratio and warm end delta temperature and a decentralized control system that conducts the regulation of the process.

Numerical studies showed that the proposed decentralized control systems for liquefaction and refrigeration units cope well with various disturbances and successfully fulfilled the tracking of large set point changes. The processes were stabilized in a relatively short transient for different scenarios in the process changes, and the product specification represented by the LNG temperature was met at all times, especially even in the case that refrigerant cold duty is not sufficient to cool and liquefy the entire feed NG. The superiority of the proposed control system was also demonstrated *via* comparison with alternative control scheme.

A special feature of the LNG process is that refrigeration and liquefaction units are closely related to each other in energy balance, while each is operated under separately-designed local controllers. To accommodate these features, the integrated control system that balances the energy supply and demand between the two units was developed. Numerical studies showed that the proposed integrated control system works quite satisfactorily, steering the process operations into the prescribed stable region.

The RTSSO was designed to minimize an objective function that consists of power consumptions in compressors. The appropriate decision variables were selected among the set points of stabilizing level loops according to the operational requirement. The objective function decreased noticeably as the optimizer updates the target operating points for the changes in disturbance value.

It is believed that the proposed optimizing control scheme has advantages over the existing ones in terms of both the optimizer and the controller performances and also the way it is implemented, real-time control and steady-state optimization. In future works, the proposed scheme will be tested on an actual 100 ton-per-day LNG plant being constructed in Incheon, Korea.

Acknowledgement

This research was supported by Basic Science Research Program through the National Research Foundation of Korea (NRF) funded by the Ministry of Education (NRF-2014R1A1A2058904).

Appendix A. Control of refrigeration unit

Figs. A1 and A2 show the controllers that utilize the DOFs of five discharge-cooler powers and one pump power in refrigeration unit, respectively. In Fig. A1, the controller tag numbers are sequentially increased.

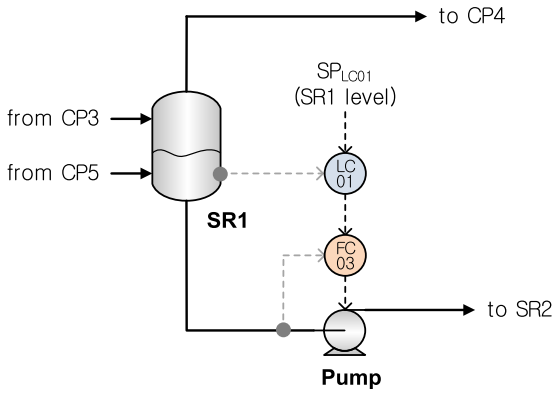

Fig. A2. Control of liquid holdup in SR1. The filled circles represent relevant measurement.

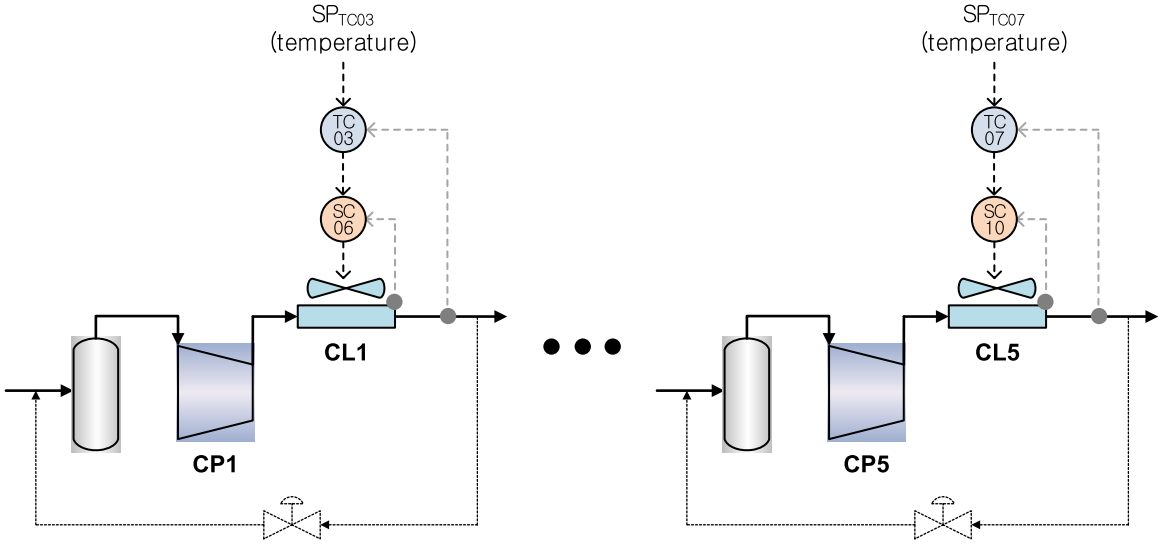

Fig. A1. Control of temperature downstream of each compressor. The filled circles represent relevant measurement.

Appendix B. Alternative control system for liquefaction unit

See Fig. B1.

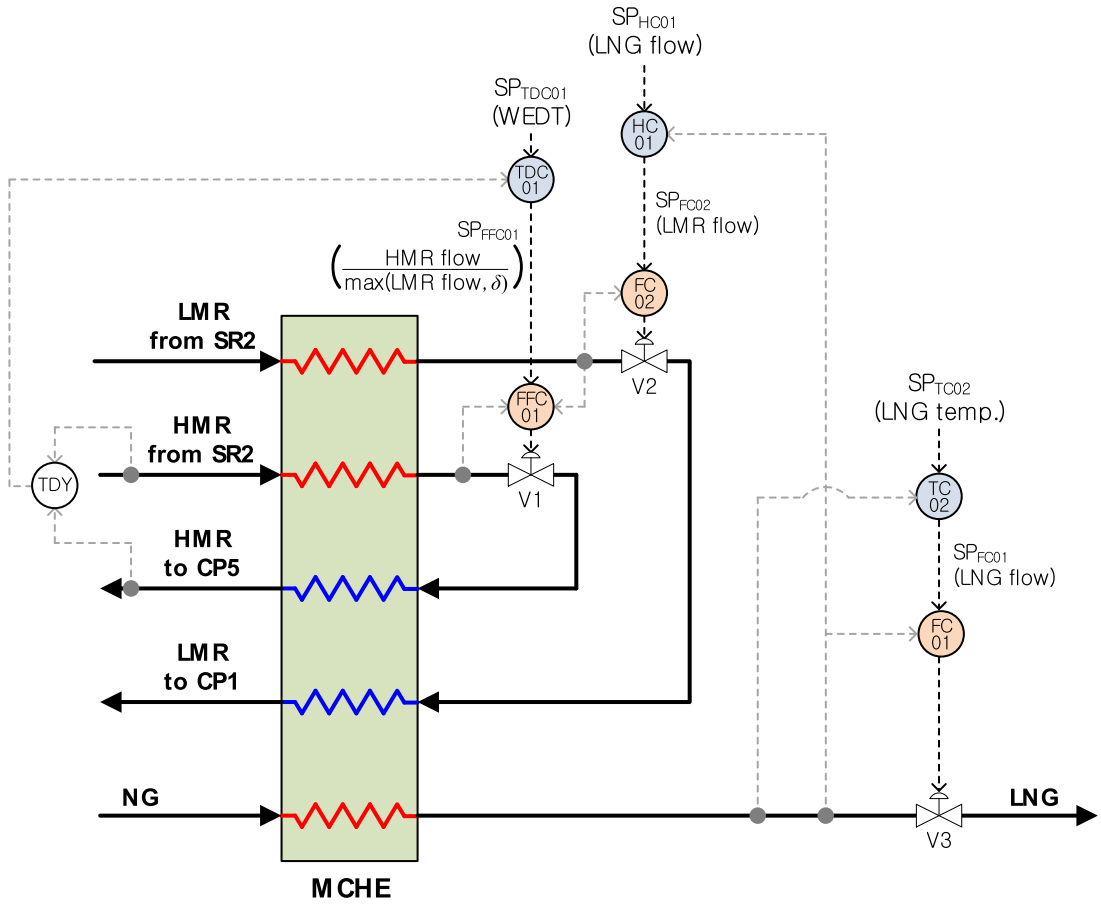

Fig. B1. Alternative control system for liquefaction unit. The filled circles represent relevant measurement.

References

Åström, K.J., Hägglund, T., 1995. PID Controllers: Theory, Design, and Tuning, 2nd ed. Instrument Society of America, NC.

Aamir, E., Nagy, Z.K., Rielly, C.D., 2010. Optimal seed recipe design for crystal size distribution control for batch cooling crystallization processes. Chem. Eng. Sci. 65, 3602–3614.

Abel, S., Erdem, G., Mazzotti, M., Morari, M., Morbidelli, M., 2005. Optimizing control of simulated moving beds – experimental implementation. J. Chromatogr. A 1092, 2–16.

Aspelund, A., Gundersen, T., Myklebust, J., Nowak, M.P., Tomasgard, A., 2010. An optimization-simulation model for a simple LNG process. Comput. Chem. Eng. 34, 1606–1617.

Bi, Q., Cai, W.J., Lee, E.L., Wang, Q.G., Hang, C.C., Zhang, Y., 1999. Robust identification of first-order plus dead-time model from step response. Control Eng. Pract. 7, 71–77.

Chang, H.M., Chung, M.J., Lee, S., Choe, K.H., 2011. An efficient multi-stage Brayton-JT cycle for liquefaction of natural gas. Cryogenics 51, 278–286.

Energy Information Administration (EIA), 2003. The Global Liquefied Natural Gas Market: Status & Outlook.

Energy Information Administration (EIA), 2005. International Energy Outlook.

Gómez, M.R., Garcia, R.F., Gómez, J.R., Carril, J.C., 2014. Review of thermal cycles exploiting the exergy of liquefied natural gas in the regasification process. Renew. Sustain. Energy Rev. 38, 781–795.

He, T., Ju, Y., 2014. Design and optimization of a novel mixed refrigerant cycle integrated with NGL recovery process for small-scale LNG plant. Ind. Eng. Chem. Res. 53, 5545–5553.

He, T., Ju, Y., 2016. Dynamic simulation of mixed refrigerant process for small-scale LNG plant in skid mount packages. Energy 97, 350–358.

Hu, W., Cai, W.J., Xiao, G., 2010. Decentralized control system design for MIMO processes with integrators/differentiators. Ind. Eng. Chem. Res. 49, 12521–12528.

Husnil, Y.A., Yeo, G., Lee, M., 2014. Plant-wide control for the economic operation of modified single mixed refrigerant process for an offshore natural gas liquefaction plant. Chem. Eng. Res. Des. 92, 679–691.

Jensen, J.B., Skogestad, S., 2007a. Optimal operation of simple refrigeration cycles. Part I: degrees of freedom and optimality of sub-cooling. Comput. Chem. Eng. 31, 712–721.

Jensen, J.B., Skogestad, S., 2007b. Optimal operation of simple refrigeration cycles. Part II: selection of controlled variables. Comput. Chem. Eng. 31, 1590–1601.

Jensen, J.B., Skogestad, S., 2009. Steady-state operational degrees of freedom with application to refrigeration cycles. Ind. Eng. Chem. Res. 48, 6652–6659.

Kanoğlu, M., 2002. Exergy analysis of multistage cascade refrigeration cycle used for natural gas liquefaction. Int. J. Energy Res. 26, 763–774.

Khan, M.S., Lee, M., 2013. Design optimization of single mixed refrigerant natural gas liquefaction process using the particle swarm paradigm with nonlinear constraints. Energy 49, 146–155.

Khan, M.S., Lee, S., Rangaiah, G.P., Lee, M., 2013. Knowledge based decision making method for the selection of mixed refrigerant systems for energy efficient LNG processes. Appl. Energy 111, 1018–1031.

Kikkawa, Y., Nakamura, M., Sugiyama, S., 1997. Development of liquefaction process for natural gas. J. Chem. Eng. Jpn. 30, 625–630.

Kiparissides, C., Seferlis, P., Mourikas, G., Morris, A.J., 2002. Online optimizing control of molecular weight properties in batch free-radical polymerization reactors. Ind. Eng. Chem. Res. 41, 6120–6131.

Klatt, K.U., Hanisch, F., Dünnebier, G., 2002. Model-based control of a simulated moving bed chromatographic process for the separation of fructose and glucose. J. Process Control 12, 203–219.

Kumar, S., Kwon, H., Choi, K., Lim, W., Cho, J.H., Tak, K., Moon, I., 2011. LNG: an eco-friendly cryogenic fuel for sustainable development. Appl. Energy 88, 4264–4273.

Lang, Y., Malacina, A., Biegler, L.T., Munteanu, S., Madsen, J.I., Zitney, S.E., 2009. Reduced order model based on principal component analysis for process simulation and optimization. Energy Fuels 23, 1695–1706.

Lee, K.S., Chin, I.S., Lee, J.H., 1999. Model predictive control technique combined with iterative learning for batch processes. AIChE J. 45, 2175–2187.

Lee, G.C., Smith, R., Zhu, X.X., 2002. Optimal synthesis of mixed-refrigerant systems for low-temperature processes. Ind. Eng. Chem. Res. 41, 5016–5028.
Lee, S., Long, N.V.D., Lee, M., 2012. Design and optimization of natural gas liquefaction and recovery processes for offshore floating liquefied natural gas plants. Ind. Eng. Chem. Res. 51, 10021–10030.
Lee, S.G., Choe, K.H., Yang, Y.M., Lee, C.G., Cha, K.S., Park, C.W., Choi, S.H., Lee, Y.B., 2013. Natural gas liquefaction process. *US patent*, US20130133362A1, USA.
Lei, Z., Yi, C., Yang, B., 2013. Design, optimization, and control of reactive distillation column for the synthesis of tert-amyl ethyl ether. Chem. Eng. Res. Des. 91, 819–830.
Li, Q.Y., Ju, Y.L., 2010. Design and analysis of liquefaction process for offshore associated gas resources. Appl. Therm. Eng. 30, 2518–2525.
Ma, D.L., Tafti, D.K., Braatz, R.D., 2002. Optimal control and simulation of multidimensional crystallization processes. Comput. Chem. Eng. 26, 1103–1116.
Mandler, J.A., 2000. Modelling for control analysis and design in complex industrial separation and liquefaction processes. J. Process Control 10, 167–175.
Michelsen, F.A., Halvorsen, I.J., Lund, B.F., Wahl, P.E., 2010. Modeling and simulation for control of the TEALARC liquefied natural gas process. Ind. Eng. Chem. Res. 49, 7389–7397.
Mizoguchi, A., Marlin, T.E., Hrymak, A.N., 1995. Operations optimization and control design for a petroleum distillation process. Can. J. Chem. Eng. 73, 896–907.
Moein, P., Sarmad, M., Ebrahimi, H., Zare, M., Pakseresht, S., Vakili, Z., 2015. APCI-LNG single mixed refrigerant process for natural gas liquefaction cycle: analysis and optimization. J. Nat. Gas Sci. Eng. 26, 470–479.
Morosuk, T., Tesch, S., Hiemann, A., Tsatsaronis, G., Omar, N.B., 2015. Evaluation of the PRICO liquefaction process using exergy-based methods. J. Nat. Gas Sci. Eng. 27, 23–31.
Mortazavi, A., Somers, C., Hwang, Y., Radermacher, R., Rodgers, P., Hashimi, S., 2012. Performance enhancement of propane pre-cooled mixed refrigerant LNG plant. Appl. Energy 93, 125–131.
Nagy, Z.K., Braatz, R.D., 2012. Advances and new directions in crystallization control. Annu. Rev. Chem. Biomol. Eng. 3, 55–75.
Natarajan, S., Lee, J.H., 2000. Repetitive model predictive control applied to a simulated moving bed chromatography system. Comput. Chem. Eng. 24, 1127–1133.
Nogal, F.D., Kim, J.K., Perry, S., Smith, R., 2008. Optimal design of mixed refrigerant cycles. Ind. Eng. Chem. Res. 47, 8724–8740.
Park, K., Won, W., Shin, D., 2016. Effects of varying the ambient temperature on the performance of a single mixed refrigerant liquefaction process. J. Nat. Gas Sci. Eng. 34, 958–968.
Remeljej, C.W., Hoadley, A.F.A., 2006. An exergy analysis of small-scale liquefied natural gas (LNG) liquefaction processes. Energy 31, 2005–2019.
Rewagad, R.R., Kiss, A.A., 2012. Dynamic optimization of a dividing-wall column using model predictive control. Chem. Eng. Sci. 68, 132–142.
Rodríguez, M., Diaz, M.S., 2007. Dynamic modelling and optimization of cryogenic systems. Appl. Therm. Eng. 27, 1182–1190.
Seborg, D.E., Mellichamp, D.A., Edgar, T.F., Doyle, F.J., 2010. Process Dynamics and Control, 3rd ed. John Wiley & Sons, New York.
Seo, S.T., Won, W., Lee, K.S., Jung, C., Lee, S., 2007. Repetitive control of Catofin process. Korean J. Chem. Eng. 24, 921–926.
Singh, A., Hovd, M., 2007. Dynamic modeling and control structure design for a liquefied natural gas process. Proceedings of American Control Conference, 1347–1352.
Skogestad, S., 2003. Simple analytic rules for model reduction and PID controller tuning. J. Process Control 13, 291–309.
Taylor, R., Tertzakian, P., Wall, T., Graham, M., Young, P.J., Harbinson, S., 2012. Natural gas: the green fuel of the future. J. Can. Pet. Technol. 51, 163–175.
Vatani, A., Mehrpooya, M., Palizdar, A., 2014. Advanced exergetic anlaysis of five natural gas liquefaction processes. Energy Convers. Manage. 78, 720–737.
Wang, M., Zhang, J., Xu, Q., 2012. Optimal design and operation of a C3MR refrigeration system for natural gas liquefaction. Comput. Chem. Eng. 39, 84–95.
Won, W., Yun, W., Ji, S.H., Na, B.C., Lee, K.S., 2009. Combined run-to-run and LQG control of a 12-inch RTP equipment. Korean J. Chem. Eng. 26, 1453–1460.
Won, W., Lee, K.S., Lee, S., Jung, C., 2010. Repetitive control and online optimization of Catofin propane process. Comput. Chem. Eng. 34, 508–517.
Won, W., Lee, S.K., Choi, K., Kwon, Y., 2014. Current trends for the floating liquefied natural gas (FLNG) technologies. Korean J. Chem. Eng. 31, 732–743.
Xu, X., Liu, J., Jiang, C., Cao, L., 2013. The correlation between mixed refrigerant composition and ambient conditions in the PRICO LNG process. Appl. Energy 102, 1127–1136.